analytical chemistry

Article

Cite This: Anal. Chem. XXXX, XXX, XXX−XXX

pubs.acs.org/ac

Target-Induced 3D DNA Network Structure as a Novel Signal Amplifier for Ultrasensitive Electrochemiluminescence Detection of MicroRNAs

Yue Zhang, Yaqin Chai, Haijun Wang,* and Ruo Yuan*

Key Laboratory of Luminescence and Real-Time Analytical Chemistry (Southwest University), Ministry of Education, College of Chemistry and Chemical Engineering, Southwest University, Chongqing 400715, People's Republic of China

Supporting Information

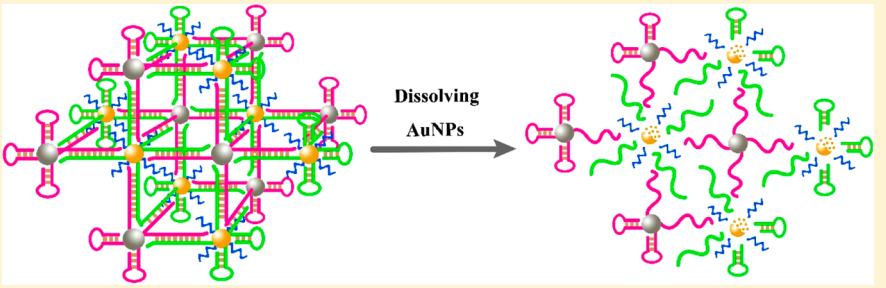

ABSTRACT: Here, a target-induced three-dimensional DNA network structure (T-3D Net) produced by catalytic hairpin assembly (CHA) was proposed as a novel signal amplifier to fabricate an ultrasensitive electrochemiluminescence (ECL) biosensor for microRNAs detection. Usually, conventional CHA can produce only one output DNA in each target cycle, while the proposed strategy could produce multiple output DNA by using DNA-functionalized magnetic beads (MBs) and gold nanoparticles (AuNPs) to form T-3D Net. Then, the T-3D Net with high loading capacity could be completely collapsed by dissolving AuNPs to efficiently convert trace microRNA-21 into a large amount of output DNA. Furthermore, the nanocomposite containing $Ru(bpy)_3^{2+}$ as luminophore and boron nitride quantum dots (BNQDs) as coreactant provided a strong initial ECL response owing to the short electron transfer distance between luminophore and coreactant (signal-on). Next, the DNA duplex probes labeled with *N*-(4-aminobutyl)-*N*-ethylisoluminol (ABEI) and dopamine (DA) (S1-ABEI/S2-DA) were further immobilized on the nanocomposite to reduce the background signal due to the double quenching effect of DA for both ABEI and $Ru(bpy)_3^{2+}$ (signal-off). In the presence of the output DNA with enzyme-assisted self-recycling, S2-DA was displaced and detached from the electrode surface to achieve ECL signal recovery. Simultaneously, S1-ABEI restored a stable hairpin structure, making ABEI close to the electrode surface for more effective resonance energy transfer (RET) between ABEI and $Ru(bpy)_3^{2+}$, which greatly improved the final ECL response (signal-super on). Thus, the ECL biosensor demonstrated superior performance for ultrasensitive detection of microRNA-21 with low detection limit (0.33 aM) and was successfully applied to monitor the expression of microRNA-21 in human cancer cell lysates. This strategy provided an ultrasensitive way for the detection of biomolecules and revealed an effective avenue for diseases diagnosis.

Electrochemiluminescence (ECL) has been widely used as a reliable analytical tool for the clinical detection of small molecules, proteins, DNA, and cells because of its low background, high sensitivity, simple device, good spatial resolution, and good temporal resolution.[1−4] In particular, $Ru(bpy)_3^{2+}$ and its derivatives have been widely used as luminophores in the ECL field,[5−7] and tripropylamine (TPrA) has been successfully used as their typical commercial coreactant.[8] However, TPrA itself has certain defects such as corrosivity, toxicity, and volatility.[9] Therefore, researchers have invested a lot of effort in developing environmental friendly coreactants. For example, Wang et al. observed that boron nitride quantum dots (BNQDs) in solution strongly enhanced the ECL intensity of $Ru(bpy)_3^{2+}$ and found it to be an efficient coreactant.[10] Besides, BNQDs as an ideal green coreactant had the advantages of good solubility, good biocompatibility, easy synthesis, low cost, and high chemical stability, which made it have a wide application. However, the long electron transfer distance between BNQDs in the solution and $Ru(bpy)_3^{2+}$ on the electrode resulted in a decrease in ECL efficiency. Hence, a nanocomposite was successfully prepared by dispersing $Ru(bpy)_3^{2+}$ and BNQDs in Nafion solution containing Pt nanoparticles (PtNPs) (BNQDs/Ru/PtNPs/Nafion), which not only had high ECL efficiency because of the shorter electron transfer distance between BNQDs and $Ru(bpy)_3^{2+}$ but also had excellent film formation and outstanding DNA

Received: June 21, 2019
Accepted: October 17, 2019
Published: October 17, 2019

DOI: 10.1021/acs.analchem.9b02817
Anal. Chem. XXXX, XXX, XXX−XXX

Scheme 1. Proposed Nucleic Acid Amplification Mechanism (A) and Construction of the Proposed ECL Biosensor (B)

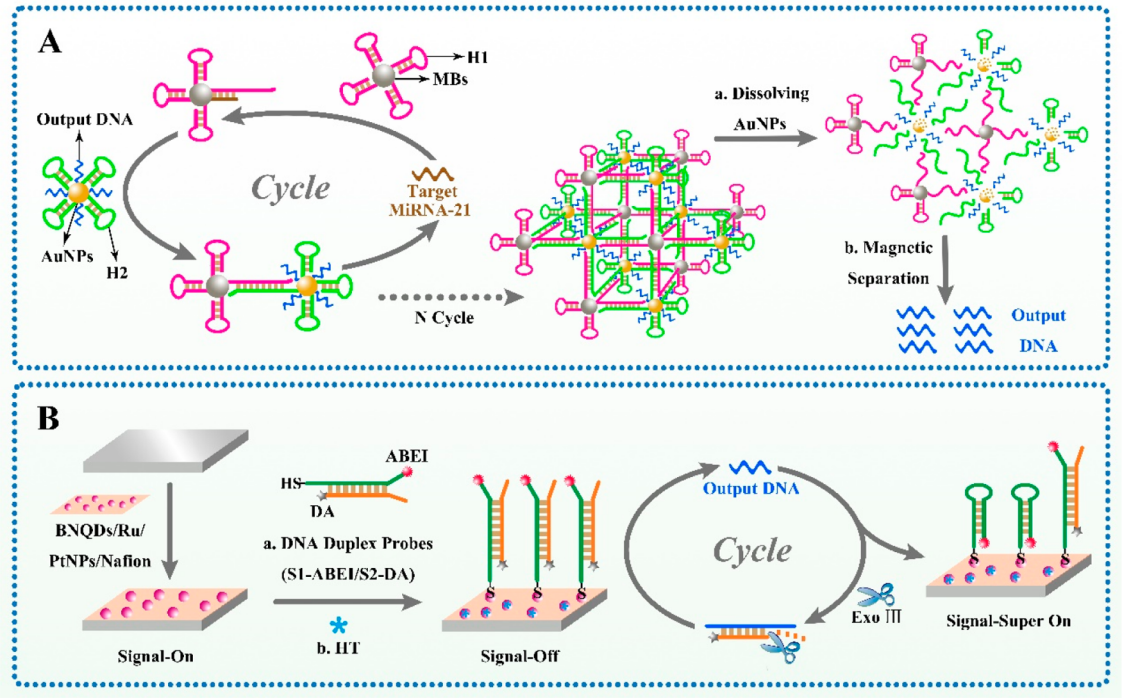

immobilization ability for the subsequent construction of the proposed biosensor.

Studies have found that microRNAs (miRNAs) are a family of endogenous and small (about 18−25 nucleotides) carcinogenic noncoding RNAs, which have played a rather important role in the development of tumors.[11−14] The need to increase the detection sensitivity of miRNAs has been quite intense because of the low abundance of miRNAs and trace levels in biological samples. Currently, nucleic acid amplification technologies have become a powerful and popular tool for signal amplification. Additionally, the widely used nucleic acid amplification strategies include catalytic hairpin assembly (CHA),[15,16] rolling circle amplification (RCA),[17] hybridization chain reaction (HCR),[18] loop-mediated isothermal amplification (LAMP),[19] polymerase chain reaction (PCR),[20] strand displacement amplification (SDA),[21] and so on. Among them, CHA as a constant temperature, enzyme-free, and low-cost amplification strategy[22,23] has achieved signal amplification through hairpin structure self-assembly and strand displacement reaction, which has attracted special attention. However, the amplification efficiency of conventional CHA is still insufficient because of the production of only one output DNA in each target cycle. Therefore, target-induced three-dimensional DNA network structure (T-3D Net) based on the CHA process was designed as a novel signal amplifier for ultrasensitive detection of miRNA-21. Compared with conventional CHA, this strategy based on DNA-functionalized nanoparticles could produce multiple output DNA in each target cycle. After multiple target cycles, T-3D Net with high loading capacity was formed, which greatly improved the detection sensitivity of miRNA-21.

Target conversion has been a commonly used method in the construction of ultrasensitive biosensor, which was more convenient for detection and efficient for signal amplification.[24] Target conversion is typically performed by enzymatic cleavage and ionic cleavage.[25,26] However, both of these methods have the disadvantage of low cleavage efficiency, resulting in insufficient conversion efficiency of the target.[27,28] In this work, the proposed T-3D Net could be rapidly and completely collapsed by dissolving gold nanoparticles (AuNPs) with use of I_2−KI-H_2O_2 solution[29] to efficiently release a large amount of output DNA, in which the target conversion efficiency could be significantly improved, producing a large amount of output DNA. Interestingly, the released output DNA not only realized the quencher detachment but also regulated the distance for resonance energy transfer (RET), resulting in significant amplification of the signal.

Herein, T-3D Net based on the CHA process was designed as a unique signal amplifier, which could efficiently convert trace miRNA-21 into a large amount of output DNA for ultrasensitive detection of miRNA-21. The proposed nucleic acid amplification mechanism and the construction of the biosensor were depicted in Scheme 1. For Process A, target miRNA-21 opened H1 modified on magnetic beads, and then H2 on H2-AuNPs-output DNA replaced miRNA-21. The released miRNA-21 then entered the next cycle to open the next H1. By analogy, T-3D Net consisting of multiple MBs-H1/H2-AuNPs-output DNA was successfully prepared. After magnetic separation, I_2−KI-H_2O_2 was added to dissolve AuNPs, which caused the T-3D Net to completely collapse and efficiently release a large amount of output DNA. For the electrode modification in Process B, the luminescent nanocomposite produced a strong initial ECL response because of the short electron transfer distance between coreactant BNQDs and luminophore $Ru(bpy)_3^{2+}$ (signal-on). Next, DNA duplex probes labeled with *N*-(4-aminobutyl)-*N*-ethylisoluminol (ABEI) and dopamine (DA) (S1-ABEI/S2-DA) were immobilized on the nanocomposite. The ECL response was significantly reduced to obtain a lower background signal because of the double quenching effect of DA for both ABEI and $Ru(bpy)_3^{2+}$ (signal-off). In the presence of the output DNA, S2-DA was displaced and detached from the electrode

DOI: 10.1021/acs.analchem.9b02817
Anal. Chem. XXXX, XXX, XXX−XXX

surface to achieve ECL signal recovery. Simultaneously, S1-ABEI restored a stable hairpin structure, which shortened the distance between ABEI (energy donor) and $Ru(bpy)_3^{2+}$ (energy acceptor), resulting in more effective RET. Moreover, the output DNA could be released by enzyme cleavage and continue to participate in the next cycle, further realizing the amplification of the signal (signal-super on). Therefore, the development of this "on−off−super on" biosensor provided a simple and effective method for the ultrasensitive detection of miRNAs, improving diagnostic efficiency of diseases.

EXPERIMENTAL SECTION

Preparation of BNQDs/Ru/PtNPs/Nafion. We synthesized BNQDs by using a one-step bottom-up hydrothermal method according to the published reports with minor modifications.[30,31] First, 0.6 g of boric acid was added to 15 mL of distilled water for dissolution, followed by the addition of 5.6 mL of concentrated ammonia and degassing with nitrogen for 20 min. Then, it was heated in an autoclave at 200 °C for 12 h, and the obtained BNQDs were stored in the dark at 4 °C before use. Ru/PtNPs aggregates were synthesized on the basis of the previous literature with some modifications.[32] Briefly, 0.5 mL of 3-thiophenemalonic acid (TA, 0.3 M) was slowly added into 50 mL of H_2PtCl_6 (0.75 mM) solution, and then the above yellow solution was heated to 100 °C for 20 min with vigorous stirring until it turned into a dark brown solution. After that, 1 mL of $Ru(bpy)_3Cl_2$ (0.038 M) aqueous solution was added into the above PtNPs colloid solution slowly with vigorous stirring until a large quantity of black aggregates occurred and precipitated. Finally, the previously prepared BNQDs and 1 mL of Nafion solution (5%, wt/wt) were added to Ru/PtNPs with stirring, and the BNQDs/Ru/PtNPs/Nafion nanocomposite was prepared.

Formation of T-3D Net and Preparation of Output DNA. First, we prepared MBs-H1 and H2-AuNPs-output DNA in advance, and the preparation process is shown in the Supporting Information. Next, 100 μL of MBs-H1 and 100 μL of different concentrations of miRNA-21 were mixed and incubated in an oven at 37 °C for 2 h to form MBs-H1-miRNA-21. Afterward, the MBs-H1-miRNA-21 was magnetically separated and rinsed three times with 100 μL of TE buffer. Then, 100 μL of H2-AuNPs-output DNA solution was added into the solution of the obtained MBs-H1-miRNA-21 and reacted in an oven at 37 °C for 2 h, thereby forming the T-3D Net. The T-3D Net was next magnetically separated and carefully rinsed three times to remove the unreacted H2-AuNPs-output DNA and finally resuspended in 100 μL of TE buffer. The T-3D Net was mixed with 30 μL of I_2-KI-H_2O_2 solution for 8 min, which caused the dissolution of AuNPs to make T-3D Net completely collapse and efficiently release a large amount of output DNA. Finally, the supernatant was efficiently collected by magnetic separation to obtain output DNA.

Fabrication of the Proposed ECL Biosensor. The preparation of the biosensor is given in Process B of Scheme 1. Prior to use, GCE requires pretreatment, and the specific experimental procedures can be found in previous studies.[33] The well-prepared GCE should be immediately used for ECL biosensor fabrication. Simultaneously, S1-ABEI/S2-DA was prepared, and the procedure is shown in Supporting Information. For GCE modification, 10 μL of BNQDs/Ru/PtNPs/Nafion was first dropped on the GCE surface and dried at 37 °C for 1 h to form a film. Afterward, 10 μL of S1-ABEI/S2-DA was incubated on the BNQDs/Ru/PtNPs/Nafion overnight at 4 °C to ensure that it was immobilized on the material. Subsequently, in order to remove nonspecific DNA adsorption, the modified GCE was blocked with 10 μL of 1 mM hexanethiol (HT) for 1 h. Following that, DNA hybridization buffer containing Exo III (2 U/μL) and 10 μL of the above output DNA was dripped onto the electrode surface and incubated at 37 °C for 1 h to effect a strand displacement reaction.

RESULTS AND DISCUSSION

Characterization of BNQDs. BNQDs were characterized by HRTEM, AFM, and fluorescence. It can be seen from the HRTEM image of Figure 1 that BNQDs were uniformly

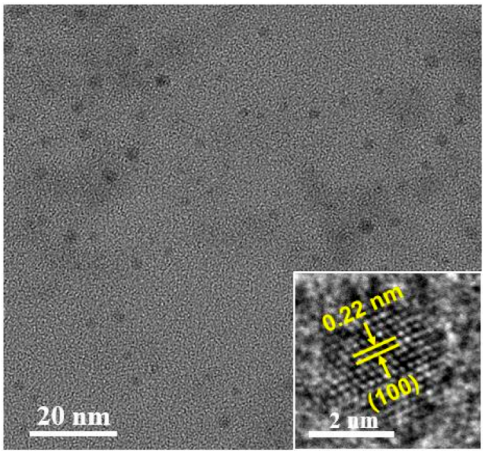

Figure 1. HRTEM image of the BNQDs. Inset: lattice fringe image.

dispersed and had a particle diameter of about 2 nm. The lattice parameter of a single BNQDs in the inset of Figure 1 was 0.22 nm and corresponded to the (100) lattice fringes of h-BN, which showed its good crystallinity. As shown in Figure 2, the AFM measurements showed that the height of the BNQDs was about 1.0 nm, indicating its monolayered structure. A typical fluorescence spectrum is shown in Figure S1A. Two excitation peaks were observed at 240 and 320 nm for BNQDs, and the maximum emission peak appeared at 410 nm. In addition, Figure S1B shows that BNQDs revealed an emission behavior unrelated to excitation as the excitation wavelength changes and was in agreement with that of the related literature.[34] All of the above morphological and optical characterizations indicated successful preparation of BNQDs. Furthermore, in order to obtain a strong and stable initial ECL intensity, we compared the ECL behaviors of three different nanocomposites (Figure S2). It was finally found that the ECL intensity of BNQDs/Ru/PtNPs/Nafion containing luminophore and coreactant was the strongest because of the short electron transfer distance.

ECL, CV, EIS, and Polyacrylamide Gel Electrophoresis (PAGE) Characterization of the Proposed Biosensor. We characterized the proposed biosensor by ECL. In Figure 3, a nanocomposite BNQDs/Ru/PtNPs/Nafion modified electrode had a strong ECL behavior because BNQDs acted as coreactant and could improve ECL intensity of $Ru(bpy)_3^{2+}$ (signal-on, curve a). When DNA duplex probes were introduced, a sharp decrease of ECL intensity was found because of the distinct double quenching effect of DA (labeled

DOI: 10.1021/acs.analchem.9b02817
Anal. Chem. XXXX, XXX, XXX−XXX

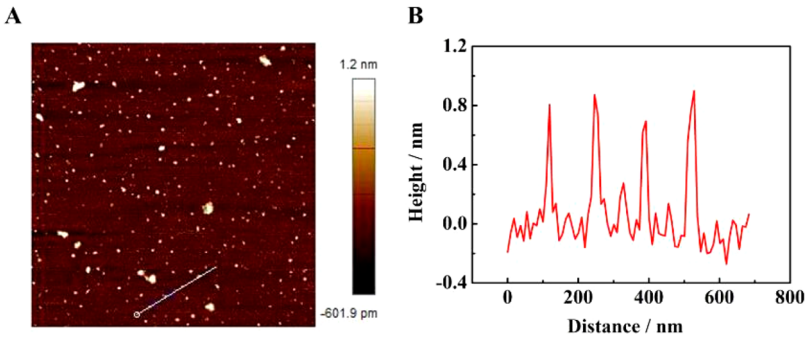

Figure 2. (A) AFM characterization of the BNQDs. (B) A height profile of the white line in panel A.

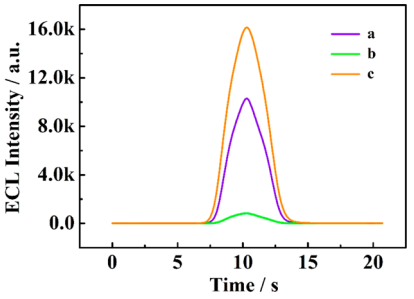

Figure 3. ECL curves of biosensor construction process: GCE/(BNQDs/Ru/PtNPs/Nafion) (a), GCE/(BNQDs/Ru/PtNPs/Nafion)/duplex probes/HT (b), GCE/(BNQDs/Ru/PtNPs/Nafion)/duplex probes/HT/output DNA (c).

on the S2) for both $Ru(bpy)_3^{2+}$ and ABEI (labeled on the S1) (signal-off, curve b). After adding output DNA, the strand displacement reaction occurred between output DNA and DNA duplex probes and the product output DNA-S2-DA left from the GCE surface. Meanwhile, S1-ABEI formed a hairpin structure, which shortened the distance between ABEI (energy donor) and $Ru(bpy)_3^{2+}$ (energy acceptor) for more effective RET. The detachment of the quencher DA and the regulation of the distance achieved a significant increase in the ECL signal. After addition of Exo III, S2-DA could be cleaved and the output DNA could be recycled to further amplify the ECL signal (signal-super on, curve c).

To further validate the feasibility of the proposed biosensing strategy, CV and EIS measurements were also carried out in $[Fe(CN)_6]^{3-/4-}$ solution (5.0 mM). It could be revealed in Figure 4A that a pair of significant $[Fe(CN)_6]^{3-/4-}$ redox peaks appeared for the bare GCE (curve a). After modification of BNQDs/Ru/PtNPs/Nafion, the redox peaks declined distinctly on account of the inhibitory effect of Nafion on electron transport, demonstrating that the nanocomposite was successfully immobilized on GCE (curve b). When DNA duplex probes, HT, and output DNA were sequentially incubated on the GCE, a gradual decrease of redox current was observed. The reason was that the immobilization of the nucleic acid and the blocking of the nonspecific binding sites by HT attenuated electrons transfer (curves c to e). Simultaneously, EIS results also confirmed the successful modification of the electrode and the electron transfers resistance (R_{et}) was calculated accurately based on the equivalent circuit with model impedance data (inset of Figure 5B). First, a small semicircle of bare GCE was observed in Figure 4B (curve a). As expected, the R_{et} increased significantly as Nafion blocked the transfer of electrons after BNQDs/Ru/PtNPs/Nafion was modified on the GCE surface (curve b). R_{et} maintained a continuous increase when DNA duplex probes, HT, and output DNA were successively immobilized onto the GCE, and the reason was that the electron transfer was hindered (curves c to e). Simultaneously, the 16% PAGE analysis was carried out to corroborate the feasibility of the strategy and the interactions among these DNA sequences (Figure S3). For the analysis of Processes A and B, the DNA reaction of each step was consistent with the strategy we designed.

ECL Detection of miRNA-21. We detected the ECL response of miRNA-21 with different concentrations under the optimal experimental conditions to investigate the performance of the obtained biosensor (Figure S5), and the feasibility of this strategy was further verified. The ECL signals were sequentially enhanced as the concentration of miRNA-21 increased (Figure 5A, curves a to g, 1 aM to 100 pM). Interestingly, the logarithm of miRNA-21 concentration showed a significant linear relationship with ECL intensity of

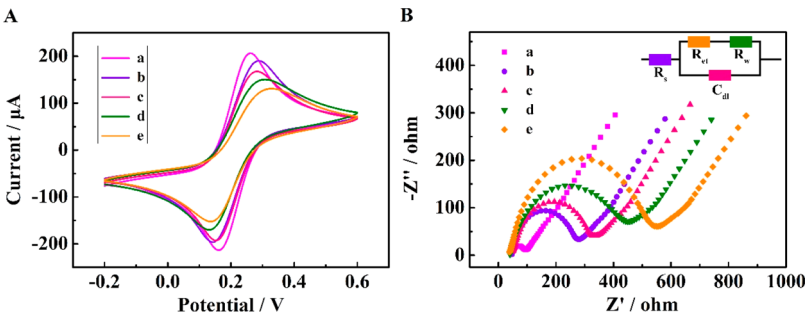

Figure 4. (A) CVs and (B) EIS curves of bare GCE (a), GCE/(BNQDs/Ru/PtNPs/Nafion) (b), GCE/(BNQDs/Ru/PtNPs/Nafion)/duplex probes (c), GCE/(BNQDs/Ru/PtNPs/Nafion)/duplex probes/HT (d), GCE/(BNQDs/Ru/PtNPs/Nafion)/duplex probes/HT/output DNA (e). Inset: the equivalent circuit with model impedance data of EIS responses.

DOI: 10.1021/acs.analchem.9b02817
Anal. Chem. XXXX, XXX, XXX−XXX

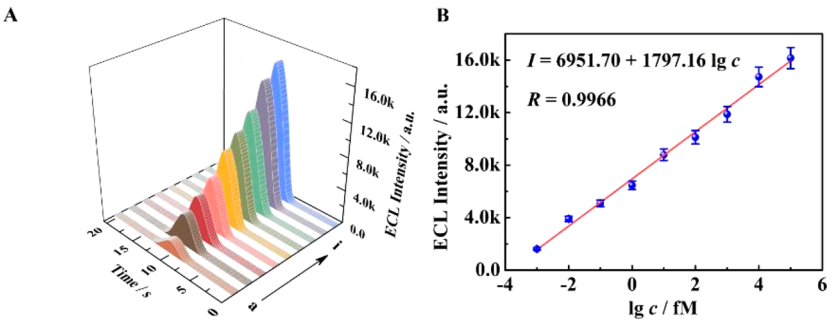

Figure 5. (A) ECL responses of biosensor with different concentrations of miRNA-21:1 aM (a), 10 aM (b), 100 aM (c), 1 fM (d), 10 fM (e), 100 fM (f), 1 pM (g), 10 pM (h) and 100 pM (i). (B) Linear relationship between the logarithm concentration of miRNA-21 and ECL intensity.

I = 6951.70 + 1797.16 lg c (I replaced the ECL intensity and c replaced the concentration of miRNA-21) and a correlation coefficient of 0.9966 in Figure 5B. Meanwhile, the limit of detection (LOD) and the limit of quantitation (LOQ) were calculated to be 0.33 aM and 1 aM according to LOD = $3S_B/m$ and LOQ = $10S_B/m$, respectively, and Figure S6 showed the specific calculation process. In addition, the added error bars were the standard deviation of eight repetitive experiments. More importantly, the performance comparison between the obtained biosensor and the previous reports illustrated that the biosensor possessed a higher sensitivity and lower LOD, which testified the potential of this biosensor in bioassay (Table 1).[35−40]

Table 1. Comparison of Proposed Assay with Reported Works for Determination of miRNA

detection methods	linear range	LOD	reference
fluorescence	1 fM to 10 pM	0.72 fM	35
fluorescence	20 pM to 10 nM	8 pM	36
electrochemical	0.10 nM to 10.0 nM	5 pM	37
electrochemical	0.1 fM to 10 nM	33 aM	38
ECL	10 fM to 0.1 nM	6.6 fM	39
ECL	10 fM to 90 fM	3.0 fM	40
ECL	1.0 aM to 100 pM	0.33 aM	this work

ECL Performance of the Target Biosensor. Biosensor stability with different concentration of miRNA-21 (100 aM and 100 fM) was evaluated by continuous cyclic potential scanning (Figure 6). When the scan was repeated 20 times, we found no discoverable changes in ECL response, indicating

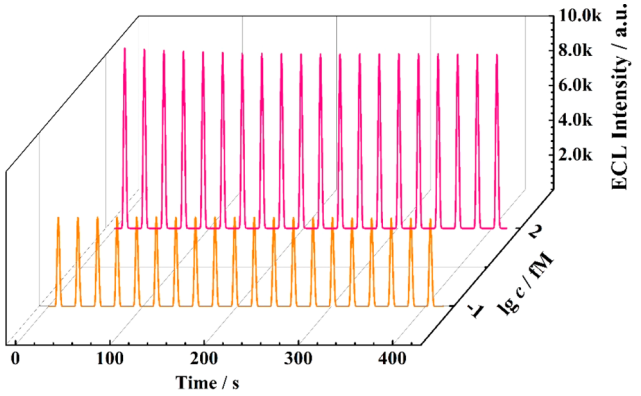

Figure 6. Stability of the target biosensor modified with 100 aM and 100 fM miRNA-21 under 20 repetitive cyclic potential scans.

that the obtained biosensor had excellent performance and good development prospects in the field of ECL biological assay.

Subsequently, considering the selectivity was another important criterion for researching sensor performance, we made further exploration. The specific detection of miRNA-21 by the obtained biosensor was confirmed by exploring the ECL responses of two interferences (miRNA-155 and miRNA-141). From the results in Figure 7, the ECL responses of interfering

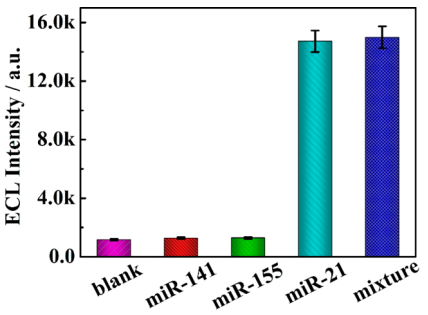

Figure 7. Selectivity of the biosensor toward miRNA-21 determination: blank, miRNA-141 (100 pM), miRNA-155 (100 pM), miRNA-21 (10 pM), and the mixture containing miRNA-21 (10 pM). The error bars were the standard deviation of eight repetitive experiments.

miRNAs (100 pM miRNA-155 and 100 pM miRNA-141) were not significantly different from that of the blank group and were obviously lower than that of the 10 pM miRNA-21. Furthermore, the ECL response of a mixture solution of the above three miRNAs (10 pM miRNA-21 containing 100 pM miRNA-155 and 100 pM miRNA-141) was close to the ECL intensity of 10 pM miRNA-21. The high selectivity could be attributed to the fact that the sequence of the target miRNA-21 specifically recognized the hairpin probe H1 in this system. Therefore, the detection method had perfect accuracy and specificity and showed excellent potential in clinical detection.

Application. In order to confirm the practical applicability of the obtained biosensor in actual samples, we specifically investigated lysates of MCF-7 (human breast cancer cells) and Hela (cervical cancer cells). The feasibility and sensitivity of the target biosensor were explored via increasing the lysate concentrations after cell counts changed from 10 to 10^5. It could be seen in Figure 8 that the ECL responses enhanced slowly and did not differ much from the blank group as Hela cell lysate concentrations changed from 10 to 10^5, indicating that miRNA-21 was under-expressed in HeLa cells. However, when the concentrations of MCF-7 cell lysate were changed

DOI: 10.1021/acs.analchem.9b02817
Anal. Chem. XXXX, XXX, XXX−XXX

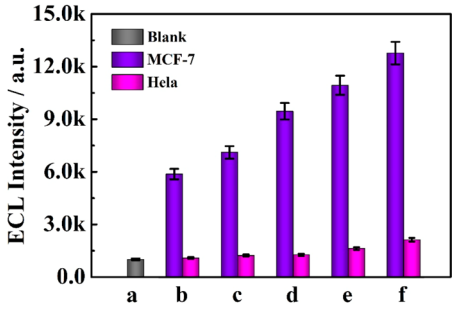

Figure 8. Analysis of miRNA-21 in MCF-7 and Hela with the obtained biosensor: blank control (a), 10 (b), 10^2 (c), 10^3 (d), 10^4 (e), and 10^5 (f) cells. The error bars were the standard deviation of eight repetitive experiments.

from 10 to 10^5, the ECL intensity was prominently enhanced, which means that miRNA-21 was highly expressed. From the above experimental results, our proposed strategy displayed good potential in quantifying the clinical diagnosis of miRNAs and diseases in tumor cells.

CONCLUSIONS

In summary, a unique signal amplifier based on T-3D Net with better loading capacity and higher amplification efficiency was designed to achieve ultrasensitive detection of miRNA-21. First, T-3D Net overcame the shortcomings of the conventional amplification strategy with insufficient loading capacity and limited amplification efficiency, which was completely collapsed by dissolving AuNPs to achieve more efficient target conversion. Second, the obtained output DNA showed multiple signal amplification effects through the target conversion. On the basis of the enzyme-assisted self-recycling, it not only completed the detachment of the quencher but also realized the distance regulation between ABEI and $Ru(bpy)_3^{2+}$, further reaching the signal amplification. Third, BNQDs had the advantages of good biocompatibility and high chemical stability as a green coreactant of luminophore $Ru(bpy)_3^{2+}$, and a prepared nanocomposite (BNQDs/Ru/PtNPs/Nafion) provided a stable and strong ECL signal owing to the short electron transfer distance between BNQDs and $Ru(bpy)_3^{2+}$. Combining the above aspects, the proposed "on−off−super on" ECL biosensor reached quantitative determination of miRNA-21 based on ultrahigh detection sensitivity and high selectivity, and obtained satisfactory results in real samples of cell lysates. Hence, this method could be applied to sensitive detection of biomarkers in clinical analysis for early diagnosis of diseases.

ASSOCIATED CONTENT

Supporting Information

The Supporting Information is available free of charge on the ACS Publications website at DOI: 10.1021/acs.analchem.9b02817.

Reagents and materials, instruments, preparation of MBs-H1, preparation of H2-AuNPs-output DNA, preparation of DNA duplex probes (S1-ABEI/S2-DA), fluorescence spectral characterization of BNQDs, ECL behaviors comparison of different luminous nanocomposites, PAGE analysis, study of the double quenching effect of DA, optimization of the ECL biosensor, calculation of LOD and LOQ (PDF)

AUTHOR INFORMATION

Corresponding Authors

*E-mail for R.Y.: yuanruo@swu.edu.cn. Tel.: +86-23-68252277. Fax: +86-23-68253172.

*E-mail for H.W.: hjwang@swu.edu.cn.

ORCID

Yaqin Chai: 0000-0003-4392-9592

Ruo Yuan: 0000-0003-3664-6236

Notes

The authors declare no competing financial interest.

ACKNOWLEDGMENTS

Thanks to the National Natural Science Foundation of China (Grant Nos. 21775124, 21575116, and 21804110), the Natural Science Foundation Project of CQ CSTC (cstc2017jcyjAX0041) and the Fundamental Research Funds for the Central Universities (XDJK2018AA003, SWU019017).

REFERENCES

(1) Feng, Y. Q.; Dai, C. H.; Lei, J. P.; Ju, H. X.; Cheng, Y. X. *Anal. Chem.* **2016**, *88*, 845−850.
(2) Ma, J.; Wu, L.; Li, Z. H.; Lu, Z. C.; Yin, W. M.; Nie, A. X.; Ding, F.; Wang, B. R.; Han, H. Y. *Anal. Chem.* **2018**, *90*, 7415−7421.
(3) Cao, W. D.; Ferrance, J. P.; Demas, J.; Landers, J. P. *J. Am. Chem. Soc.* **2006**, *128*, 7572−7578.
(4) Cui, C.; Chen, Y.; Jiang, D. C.; Chen, H. Y.; Zhang, J. R.; Zhu, J. J. *Anal. Chem.* **2019**, *91*, 1121−1125.
(5) Liu, Z. Y.; Qi, W. J.; Xu, G. B. *Chem. Soc. Rev.* **2015**, *44*, 3117−3142.
(6) Cao, J. T.; Wang, Y. L.; Zhang, J. J.; Dong, Y. X.; Liu, F. R.; Ren, S. W.; Liu, Y. M. *Anal. Chem.* **2018**, *90*, 10334−10339.
(7) Valenti, G.; Rampazzo, E.; Bonacchi, S.; Petrizza, L.; Marcaccio, M.; Montalti, M.; Prodi, L.; Paolucci, F. *J. Am. Chem. Soc.* **2016**, *138*, 15935−15942.
(8) Lu, H. J.; Pan, J. B.; Wang, Y. Z.; Ji, S. Y.; Zhao, W.; Luo, X. L.; Xu, J. J.; Chen, H. Y. *Anal. Chem.* **2018**, *90*, 10434−10441.
(9) Miao, W. J.; Choi, J. P.; Bard, A. J. *J. Am. Chem. Soc.* **2002**, *124*, 14478−14485.
(10) Xing, H. H.; Zhai, Q. F.; Zhang, X. W.; Li, J.; Wang, E. K. *Anal. Chem.* **2018**, *90*, 2141−2147.
(11) He, L.; Hannon, G. J. *Nat. Rev. Genet.* **2004**, *5*, 522−531.
(12) Li, M. X.; Zhao, W.; Wang, H.; Li, X. L.; Xu, C. H.; Chen, H. Y.; Xu, J. J. *Anal. Chem.* **2018**, *90*, 14255−14259.
(13) Ma, W.; Fu, P.; Sun, M. Z.; Xu, L. G.; Kuang, H.; Xu, C. L. *J. Am. Chem. Soc.* **2017**, *139* (34), 11752−11759.
(14) Yi, J. T.; Chen, T. T.; Huo, J.; Chu, X. *Anal. Chem.* **2017**, *89*, 12351−12359.
(15) Zhang, Y.; Li, X.; Xu, Z. Q.; Chai, Y. Q.; Wang, H. J.; Yuan, R. *Chem. Commun.* **2018**, *54*, 10148−10151.
(16) Li, B.; Ellington, A. D.; Chen, X. *Nucleic Acids Res.* **2011**, *39*, e110.
(17) Deng, R. J.; Tang, L. H.; Tian, Q. Q.; Wang, Y.; Lin, L.; Li, J. H. *Angew. Chem., Int. Ed.* **2014**, *53*, 2389−2393.
(18) Xu, G. L.; Zhao, H.; Reboud, J.; Cooper, J. M. *ACS Nano* **2018**, *12*, 7213−7219.
(19) Cai, S.; Jung, C.; Bhadra, S.; Ellington, A. D. *Anal. Chem.* **2018**, *90*, 8290−8294.
(20) Mestdagh, P.; Feys, T.; Bernard, N.; Guenther, S.; Chen, C.; Speleman, F.; Vandesompele, J. *Nucleic Acids Res.* **2008**, *36*, e143.
(21) Xue, C.; Zhang, S. X.; Ouyang, C. H.; Chang, D. R.; Salena, B. J.; Li, Y. F.; Wu, Z. S. *Angew. Chem., Int. Ed.* **2018**, *57*, 9739−9743.
(22) Jiang, Y. S.; Li, B. L.; Milligan, J. N.; Bhadra, S.; Ellington, A. D. *J. Am. Chem. Soc.* **2013**, *135*, 7430−7433.
(23) Yin, P.; Choi, H. M. T.; Calvert, C. R.; Pierce, N. A. *Nature* **2008**, *451*, 318−322.

DOI: 10.1021/acs.analchem.9b02817
Anal. Chem. XXXX, XXX, XXX−XXX

(24) Qing, M.; Xie, S. B.; Cai, W.; Tang, D. Y.; Tang, Y.; Zhang, J.; Yuan, R. *Anal. Chem.* **2018**, *90*, 11439−11445.
(25) He, M. Q.; Wang, K.; Wang, W. J.; Yu, Y. L.; Wang, J. H. *Anal. Chem.* **2017**, *89*, 9292−9298.
(26) Zhou, Y.; Wang, H. J.; Zhang, H.; Chai, Y. Q.; Yuan, R. *Anal. Chem.* **2018**, *90*, 3543−3549.
(27) Lei, Y. M.; Zhou, J.; Chai, Y. Q.; Zhuo, Y.; Yuan, R. *Anal. Chem.* **2018**, *90*, 12270−12277.
(28) Li, P. X.; Wei, M.; Zhang, F.; Su, J.; Wei, W.; Zhang, Y. J.; Liu, S. Q. *ACS Appl. Mater. Interfaces* **2018**, *10*, 43405−43410.
(29) Zhang, W. N.; Liu, Y. Y.; Lu, G.; Wang, Y.; Li, S. Z.; Cui, C. L.; Wu, J.; Xu, Z. L.; Tian, D. B.; Huang, W.; DuCheneu, J. S.; Wei, W. D.; Chen, H. Y.; Yang, Y. H.; Huo, F. W. *Adv. Mater.* **2015**, *27*, 2923−2929.
(30) Liu, B. P.; Yan, S. H.; Song, Z. Q.; Liu, M. L.; Ji, X. Q.; Yang, W. R.; Liu, J. Q. *Chem. - Eur. J.* **2016**, *22*, 18899−18907.
(31) Xing, H. H.; Zhai, Q. F.; Zhang, X. W.; Li, J.; Wang, E. K. *Anal. Chem.* **2018**, *90*, 2141−2147.
(32) Sun, X. P.; Du, Y.; Zhang, L. X.; Dong, S. J.; Wang, E. K. *Anal. Chem.* **2006**, *78*, 6674−6677.
(33) Zhang, P.; Lin, Z.; Zhuo, Y.; Yuan, R.; Chai, Y. Q. *Anal. Chem.* **2017**, *89*, 1338−1345.
(34) Dong, Y.; Pang, H.; Yang, H. B.; Guo, C.; Shao, J.; Chi, Y.; Li, C. M.; Yu, T. *Angew. Chem., Int. Ed.* **2013**, *52*, 7800−7804.
(35) Hu, J.; Liu, M. H.; Zhang, C. Y. *Chem. Sci.* **2018**, *9*, 4258−4267.
(36) Liang, C. P.; Ma, P. Q.; Liu, H.; Guo, X. G.; Yin, B. C.; Ye, B. C. *Angew. Chem., Int. Ed.* **2017**, *56*, 9077−9081.
(37) Castañeda, A. D.; Brenes, N. J.; Kondajji, A.; Crooks, R. M. *J. Am. Chem. Soc.* **2017**, *139*, 7657−7664.
(38) Xue, S. Y.; Li, Q. Q.; Wang, L.; You, W. B.; Zhang, J.; Che, R. C. *Anal. Chem.* **2019**, *91*, 2659−2666.
(39) Zhang, P.; Jiang, J.; Yuan, R.; Zhuo, Y.; Chai, Y. Q. *J. Am. Chem. Soc.* **2018**, *140*, 9361−9364.
(40) Qiao, Y. L.; Li, Y.; Fu, W.; Guo, Z. H.; Zheng, X. W. *Anal. Chem.* **2018**, *90*, 9629−9636.

DOI: 10.1021/acs.analchem.9b02817
Anal. Chem. XXXX, XXX, XXX−XXX